

# Synthesis of Supramolecular Precision Polymers: Crystallization Under Conformational Constraints

Sophie Reimann <sup>1</sup>, Varun Danke <sup>2</sup>, Mario Beiner <sup>2</sup>, Wolfgang H. Binder <sup>1</sup>

<sup>1</sup>Institute of Chemistry, Macromolecular Chemistry, Martin Luther University Halle-Wittenberg, 06120 Halle (Saale), Germany

<sup>2</sup>Fraunhofer Institut für Mikrostruktur von Werkstoffen und Systemen IMWS, 06120 Halle (Saale), Germany

Correspondence to: W. H. Binder (E-mail: wolfgang.binder@chemie.uni-halle.de)

Received 5 July 2017; accepted 9 August 2017; published online 00 Month 2017

DOI: 10.1002/pola.28759

**ABSTRACT:** Placing artificial folding elements into precision polymers is an important strategy to systematically study structure formation in self-assembly, particularly in the semicrystalline state. To this purpose, a series of precision polymers bearing either a N-protected or N-unprotected diaminopyridine (DAP) unit after every 16th, 18th, and 20th carbon as well as a urea unit after every 20th carbon along a polyethylene-like polymer were synthesized via acyclic diene metathesis polymerization and subsequent hydrogenation. The polymers thus contain either H-bonds (urea/DAP),  $\pi$ - $\pi$ -elements (DAP), or no H-bonds (respective N-protected urea/DAP-units) in their main chain, able to consequently study the crystallization behavior under influence of such supramolecular

moieties. Therefore, the thermal properties and crystallization behavior were analyzed via differential scanning calorimetry (DSC) as well as wide angle X-ray diffraction. The obtained crystalline polymer is influenced by the different supramolecular interactions existing between adjacent polymer chains and the varying defect size exerted by the incorporated functional groups. © 2017 Wiley Periodicals, Inc. *J. Polym. Sci., Part A: Polym. Chem.* **2017**, *00*, 000–000

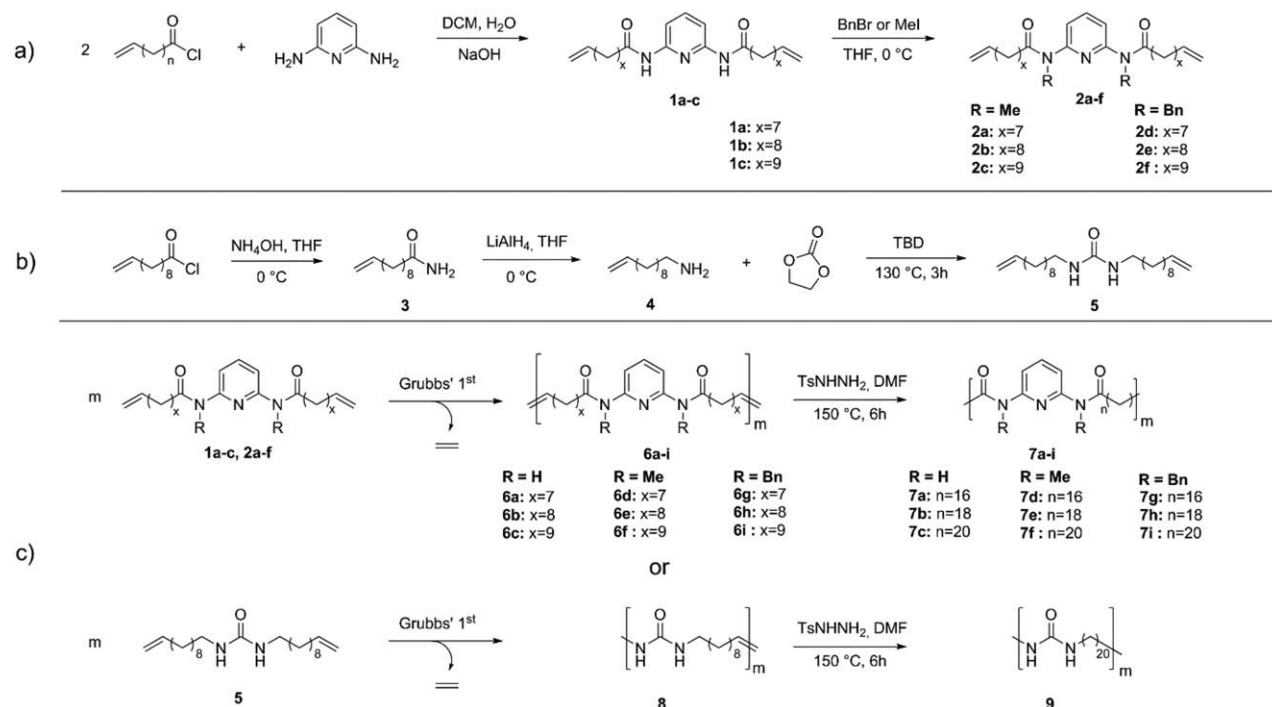
**KEYWORDS:** acyclic diene metathesis; crystallization; differential scanning calorimetry (DSC); polymer synthesis; precision polymers; supramolecular polymer chemistry; WAXS

**INTRODUCTION** The crystallization of polymers in nanoscopic domains can strongly be influenced by constraints, either exerted from the “outside” (e.g., geometrical confinement by alumina nanopores<sup>1–4</sup>) or “self-assembled constraints” occurring in two-phasic polymers, where the crystallization of one phase is strongly influenced by the second phase in the environment. Famous examples for the latter case are block copolymers, where glassy or crystalline matrices influence the crystallization of crystallizable domains with typical domain sizes of about 10–50 nm,<sup>5–7</sup> or nanophase separated polymers with comb-like architecture, where constraints introduced by ring-type subunits located in a crystalline nanolayer can disturb the crystallization behavior of long methylene sequences.<sup>8–10</sup> In case of linear polymers, where long methylene sequences alternate with functional groups (“defects”) within the polymer backbone, their incorporation or exclusion into crystalline regions has been intensively studied.<sup>11–26</sup> Especially precision polymers, resulting from acyclic diene metathesis (ADMET) polymerization<sup>27</sup> or “click”-based oligomerization chemistries,<sup>28,29</sup> have been investigated in this context, often observing a layered arrangement of defects if the included moieties interact with

each other via ionic-forces or  $\pi$ - $\pi$ -stacking as observed for polymers bearing triazol-rings,<sup>29</sup> sulfonic,<sup>30</sup> or amino acid groups in the main chain.<sup>31,32</sup> Investigation of these inclusion- or separation effects has been accomplished using long chain alkanes and their derivatives<sup>33</sup> as well as various periodic copolymers<sup>34–38</sup> differing in branch identity and frequency. Thus, in chains reminiscent of polyethylenes large defects such as higher alkyl substituents<sup>18,39</sup> (starting from propyl-branches) as well as phosphoesters<sup>12,40</sup> or polyhedral silsesquioxanes<sup>41</sup> are excluded from the crystal lattice into the interstitial space, especially if the alkyl chain length between the defects is increased.<sup>39</sup> If the excluded branch exceeds the size of 10 carbons the defects can cocrystallize,<sup>39,42</sup> also observed for polymers bearing perfluorinated chains,<sup>28</sup> where the segregation was facilitated by the immiscibility between the polymer backbone and the branch, leading to additional ordering effects on the crystallization. In contrast, small defects such as methyl<sup>39,43</sup>-, ethyl<sup>44</sup>-, or halogen<sup>11,13,45–47</sup>-branches can be incorporated into the crystalline region of the polyethylene (PE) -chains, whereby the orthorhombic structure is preserved up to a defect size of about 1.6 Å.<sup>45</sup>

Additional Supporting Information may be found in the online version of this article.

© 2017 Wiley Periodicals, Inc.



**SCHEME 1** Synthetic route for (a) the preparation of unprotected and protected DAP monomers (**1a–c**, **2a–f**), (b) the preparation of the urea monomer (**5**), and (c) the ADMET polymerization and subsequent hydrogenation.

The idea of this work is to design and investigate polymers, where folding-constraints are introduced repetitively into long methylene sequences ( $n = 16, 18$ , and  $20$ ), frustrating their folding such that the packing behavior of the methylene sequences<sup>48,49</sup> can exhibit a lamellar morphology. A recent study has shown that the methylene sequences in such polymers may be ordered or disordered depending on the thermal history as well as the length of the alkyl groups, also observing polymorphic states for the same side chain lengths.<sup>8</sup>

We here report on the synthesis of precision polymers bearing defects, which are repetitively located within a PE-chain and feature hydrogen-bonding and aromaticity as shown in Scheme 1. Thus, N-substituted 2,6-diaminopyridine-moieties (DAP) have been chosen to study the effect of H-bonds onto the crystallization behavior of the alkyl units, protecting the amides via either methyl- or benzyl units to probe the effect of bulkiness of the non-hydrogen moieties on the structure formation, whereas the absence of the protecting group should enable strong intermolecular hydrogen bonds, now acting between the chains in the crystal. Furthermore, the aromatic DAP element was replaced by a simple urea moiety, devoid of  $\pi$ - $\pi$ -stacking interactions. The synthetic preparation of the polymers and the influence of the main chain defects on the molecular ordering in the solid state are reported in detail.

## EXPERIMENTAL

Dodec-11-enoic acid, dec-9-enoyl chloride, undec-10-enoyl chloride, and dodec-11-enoyl chloride were synthesized according to literatures.<sup>37,50</sup>

All chemicals were purchased from Sigma-Aldrich and used without further purification if not mentioned otherwise. All solvents were either distilled and/or dried using standard methods.

Tetrahydrofuran (THF) was predried over KOH and freshly distilled from sodium/benzophenone under an atmosphere of dry nitrogen. Dichloromethane (DCM) was predried over  $\text{CaCl}_2$  and freshly distilled from  $\text{CaH}_2$  before use. Before using sodium hydride (60% in mineral oil), it was washed several times with dry THF and stored under an atmosphere of nitrogen.

NMR spectra were recorded in  $\text{CDCl}_3$  (Chemotrade, 99.8% Atom%D) on a Varian spectrometer (Gemini 400) at 400 MHz or on a Varian Unity Inova 500 (500 MHz) at 27 °C and tetramethylsilane as internal standard. The coupling constants were given in Hz and the chemical shifts in ppm and referred to the solvent residue peak [ $\text{CDCl}_3$  7.26 ppm ( $^1\text{H}$ ) and 77.0 ppm ( $^{13}\text{C}$ )]. MestReNova v. 8.0.0–10524 was used for the interpretation of the spectra.

Size exclusion chromatography (SEC) measurements were performed on a Viscotek GPCmax VE2001, equipped with a  $\text{GMH}_{\text{HR}}\text{-N-18055}$  and a SMT-3000 column in THF at 25–30 °C with a sample concentration of  $1 \text{ mg mL}^{-1}$ . The injection volume was 100  $\mu\text{L}$  and the detection was carried out via a refractive index detection using a VE3580 RI detector or via UV detector (model no. 2600) of Viscotek at a temperature of 35 °C and a flow rate of  $1 \text{ mL min}^{-1}$ . For external calibration, polystyrene standards with molecular weights of 1050, 2790, 6040, 13,400, and 29600  $\text{g mol}^{-1}$  were used.

Electrospray ionization-time-of-flight (ESI-ToF) mass spectrometry (MS) measurements were performed on a Focus microToF by Bruker Daltonics. The sample (1.00 mg) was dissolved in methanol (1.00 mL, HPLC grade, received from Sigma-Aldrich) and directly injected (180  $\mu\text{L h}^{-1}$ , positive or negative mode). The interpretation of the data was carried out using DataAnalysis Version 4.0 from Bruker.

Matrix-assisted laser desorption ionization (MALDI)-ToF MS measurements were performed on a Bruker Autoflex III System (Bruker Daltonics) operating in the linear and reflection mode. Ions were formed by laser desorption (smart beam laser at 355, 532, 808, and  $1064 \pm 5$  nm; 3 ns pulse width; up to 2500 Hz repetition rate), accelerated by a voltage of 19–20 kV and detected as positive ions. The matrix *trans*-2-[3-(4-*tert*-butylphenyl)-2-methyl-2-propenylidene]malononitrile (purchased from Sigma-Aldrich), the salt lithiumtrifluoroacetate (purchased from Sigma-Aldrich) as well as the polymer sample were dissolved in THF with a concentration of 20 mg mL<sup>-1</sup> each. The solutions of the matrix, the polymer, and the salt were mixed in a volume ratio of 25:5:1 and 1  $\mu\text{L}$  of each mixture was spotted on the MALDI target. Calibration was carried out with poly(ethylene glycol) monomethyl ether (PEG) ( $M_n = 4200$  g mol<sup>-1</sup>,  $M_w/M_n = 1.05$ ) as external standard. The interpretation of the data was carried out using flexAnalysis Version 3.4 (build 76) from Bruker.

Differential scanning calorimetry (DSC) measurements were performed on a NETZSCH DSC 204F1 Phoenix, which was calibrated with indium, tin, and zinc. The samples (3–8 mg) were filled in standard aluminum pans with a pierced lid, heated above their melting point, and cooled to room temperature to erase the previous thermal history. Afterwards the samples were subjected to a thermal program using a heating rate of 10 K/min. Interpretation of the obtained data was performed with Netzsch Proteus—Thermal Analysis (version 5.2.1) and OriginPro 2016G. The crystallinity  $X_c$  was calculated according to the equation given below

$$X_c = \frac{\Delta H_m}{\Delta H_m^0} \times 100 \quad (1)$$

where  $\Delta H_m^0$  is the fusion enthalpy of the corresponding alkane (hexadecane  $\Delta H_m^0 = 225.146$  J g<sup>-1</sup>, octadecane  $\Delta H_m^0 = 232.269$  J g<sup>-1</sup> or eicosane  $\Delta H_m^0 = 247.3$  J g<sup>-1</sup>) with 100% crystallinity.

Initial X-ray diffraction screening experiments for the saturated DAP-polymers with methyl protection groups ( $n = 16, 18, 20$ ) were performed on a glass plate by cooling the sample from the isotropic liquid on a temperature-controlled heating stage. The two-dimensional patterns were recorded by an area detector VÅNTEC500 (Bruker AXS) using Ni-filtered CuK $\alpha$  radiation at a sample-detector distance of 8.95 cm and an exposure time of 30 min.

X-ray scattering experiments were performed in transmission mode using a SAXSLAB laboratory setup (Retro-F) equipped with an AXO microfocus X-ray source with an AXO multilayer

X-ray optic (ASTIX) as monochromator for Cu K $\alpha$  radiation ( $\lambda = 0.154$  nm). A DECTRIS PILATUS3 R 300K detector was used to record the two-dimensional scattering patterns. As sample holders 2 mm thick aluminum discs with a central hole were used. The measurements were performed at room temperature in vacuum for three samples to detect distances to cover a wider  $q$ -range ( $q = 0.05$ – $3$  nm<sup>-1</sup>;  $0.25$ – $7$  nm<sup>-1</sup>, and  $q = 1$ – $29$  nm<sup>-1</sup>). Before the measurement the samples were annealed for 24 h at 40 °C followed by cooling them to room temperature.

Fourier-transform infrared spectroscopy (FTIR) was performed as KBr pellet on a Bruker Vertex 70 MIR using Opus 6.5 for data interpretation.

For thin-layer chromatography (TLC) Merck TLC aluminum sheets (silica gel 60 F254) were used. The resulting spots were visualized by UV light (254 nm) or by the oxidizing agent “blue stain.” This was prepared by dissolving Ce(SO<sub>4</sub>)<sub>2</sub>·4H<sub>2</sub>O and (NH<sub>4</sub>)<sub>6</sub>Mo<sub>7</sub>O<sub>24</sub>·4H<sub>2</sub>O in a mixture of distilled water and concentrated sulfuric acid.

Column chromatography was performed with Kieselgel 60 (230–400 mesh), which was received from Merck.

## Monomer Synthesis

### General Synthesis of the ADMET Monomers Containing the DAP Group

All DAP monomers were synthesized in a biphasic Schotten-Baumann reaction according to our previous investigations.<sup>51</sup> A one-necked flask was filled with 2,6-diaminopyridine (1 eq.) and NaOH (2 eq.), which were dissolved in water. The mixture was cooled in an ice-water bath and dec-9-enoyl chloride, undec-10-enoyl chloride, or dodec-11-enoyl chloride (2.3 eq.) dissolved in DCM was added slowly for 15 min. After the mixture was allowed to stir for 2 h the organic layer was separated and dried over Na<sub>2</sub>SO<sub>4</sub>. The solvent was removed in vacuum at 45 °C and the crude product was purified via column chromatography (silica gel 60, hexane/ethyl acetate (EA) 8:2) to yield a white solid (92–94%).

DAP-M-7 (**1a**): <sup>1</sup>H NMR (400 MHz, CDCl<sub>3</sub>,  $\delta$ ): 7.89 (d,  $J = 8.0$  Hz, 2H, CH), 7.68 (t,  $J = 8.1$  Hz, 1H, CH), 7.57 (s, 2H, NH), 5.93–5.65 (m, 2H, =CH), 5.08–4.82 (m, 4H, =CH<sub>2</sub>), 2.36 (t,  $J = 7.5$  Hz, 4H, CH<sub>2</sub>), 2.12–1.97 (m, 4H, CH<sub>2</sub>), 1.82–1.60 (m, 4H, CH<sub>2</sub>), 1.49–1.14 (m, 16H, CH<sub>2</sub>). <sup>13</sup>C NMR (101 MHz, CDCl<sub>3</sub>,  $\delta$ ): 171.6 (C=O), 149.5 (C3), 141.0 (C1), 139.2 (C12), 114.4 (C13), 109.5 (C2), 38.0 (C5), 33.9 (C11), 29.3 (C7), 29.3 (C8), 29.0 (C10), 29.0 (C9), 25.5 (C6). HRMS (ESI,  $m/z$ ):  $[M + Na]^+$  calcd for C<sub>25</sub>H<sub>39</sub>N<sub>3</sub>O<sub>2</sub>, 436.2934; found, 436.3250.

DAP-M-8 (**1b**): <sup>1</sup>H NMR (400 MHz, CDCl<sub>3</sub>,  $\delta$ ): 7.89 (d,  $J = 8.1$  Hz, 2H, CH), 7.69 (t,  $J = 8.1$  Hz, 1H, CH), 7.56 (s, 2H, NH), 5.96–5.66 (m, 2H, =CH), 5.09–4.84 (m, 4H, =CH<sub>2</sub>), 2.36 (t,  $J = 7.5$  Hz, 4H, CH<sub>2</sub>), 2.03 (dd,  $J = 6.8$  Hz, 4H, CH<sub>2</sub>), 1.82–1.59 (m, 4H, CH<sub>2</sub>), 1.47–1.15 (m, 20H, CH<sub>2</sub>). <sup>13</sup>C NMR (101 MHz, CDCl<sub>3</sub>,  $\delta$ ): 171.6 (C=O), 149.6 (C3), 141.0 (C1), 139.3 (C13), 114.3 (C14), 109.5 (C2), 38.0 (C5), 33.9 (C12), 29.4 (C8), 29.4 (C10), 29.3 (C9), 29.2 (C11), 29.0 (C7), 25.5 (C6).

HRMS (ESI,  $m/z$ ):  $[M + Na]^+$  calcd for  $C_{27}H_{43}N_3O_2$ , 464.3247; found, 464.3571.

DAP-M-9 (**1c**):  $^1H$  NMR (400 MHz,  $CDCl_3$ ,  $\delta$ ): 7.90 (d,  $J = 8.1$  Hz, 2H, CH), 7.69 (t,  $J = 8.1$  Hz, 1H, CH), 7.52 (s, 2H, NH), 5.90–5.72 (m, 2H, =CH), 5.05–4.87 (m, 4H, =CH<sub>2</sub>), 2.36 (t,  $J = 7.5$  Hz, 4H, CH<sub>2</sub>), 2.12–1.97 (m, 4H, CH<sub>2</sub>), 1.76–1.67 (m, 4H, CH<sub>2</sub>), 1.45–1.21 (m, 24H, CH<sub>2</sub>).  $^{13}C$  NMR (101 MHz,  $CDCl_3$ ,  $\delta$ ): 171.6 (C=O), 149.6 (C3), 141.0 (C1), 139.3 (C14), 114.3 (C15), 109.5 (C2), 38.0 (C5), 33.9 (C13), 29.6 (C8), 29.5 (C10), 29.5 (C11), 29.3 (C7), 29.2 (C9), 29.1 (C12), 25.5 (C6). HRMS (ESI,  $m/z$ ):  $[M + Na]^+$  calcd for  $C_{29}H_{47}N_3O_2$ , 492.3560; found, 492.3496.

### General Procedure for the Protection of the DAP Monomers

The protection of the amides (**1a–c**) with methyl and benzyl protection groups was carried out as reported previously.<sup>51,52</sup> A two-necked flask was filled with a solution of the unprotected monomer **1a–c** (1 eq.) and methyl iodide or benzyl bromide (2.4 eq.) in dry THF and NaH (2.4 eq.) was added portion wise at 0 °C. The reaction mixture was allowed to warm up to room temperature and was stirred overnight, followed by pouring carefully into ice water. After extraction with ethyl acetate, the combined organic layers were washed with water and dried over  $MgSO_4$ . The solvent was removed in vacuum at 45 °C and the crude product was purified via column chromatography (silica gel 60, hexane/EA 8:2) to yield pale yellow viscous oils (69–82%).

DAP-M-Me-7 (**2a**):  $^1H$  NMR (400 MHz,  $CDCl_3$ ,  $\delta$ ): 7.75 (t,  $J = 7.9$  Hz, 1H, CH), 7.24 (d,  $J = 8.4$  Hz, 2H, CH), 5.90–5.68 (m, 2H, =CH), 5.05–4.86 (m, 4H, =CH<sub>2</sub>), 3.36 (s, 6H, CH<sub>3</sub>), 2.36 (t,  $J = 7.6$  Hz, 4H, CH<sub>2</sub>), 2.01 (q,  $J = 6.9$  Hz, 4H, CH<sub>2</sub>), 1.74–1.55 (m, 4H, CH<sub>2</sub>), 1.44–1.15 (m, 16H, CH<sub>2</sub>).  $^{13}C$  NMR (101 MHz,  $CDCl_3$ ,  $\delta$ ): 173.7 (C=O), 155.0 (C3), 139.8 (C1), 139.2 (C12), 117.7 (C2), 114.3 (C13), 35.4 (C14), 35.3 (C5), 33.9 (C11), 29.4 (C7), 29.4 (C8), 29.1 (C10), 29.0 (C9), 25.4 (C6). HRMS (ESI,  $m/z$ ):  $[M + Na]^+$  calcd for  $C_{27}H_{43}N_3O_2$ , 464.3247; found, 464.3555.

DAP-M-Me-8 (**2b**):  $^1H$  NMR (400 MHz,  $CDCl_3$ ,  $\delta$ ): 7.75 (t,  $J = 8.2$  Hz, 1H, CH), 7.24 (d,  $J = 8.0$  Hz, 2H, CH), 5.93–5.68 (m, 2H, =CH), 5.04–4.86 (m, 4H, =CH<sub>2</sub>), 3.36 (s, 6H, CH<sub>3</sub>), 2.36 (t,  $J = 7.5$  Hz, 4H, CH<sub>2</sub>), 2.12 (dd,  $J = 7.3$  Hz,  $J = 1.6$  Hz, 4H, CH<sub>2</sub>), 1.72–1.55 (m, 4H, CH<sub>2</sub>), 1.43–1.17 (m, 20H, CH<sub>2</sub>).  $^{13}C$  NMR (101 MHz,  $CDCl_3$ ,  $\delta$ ): 173.7 (C=O), 155.0 (C3), 139.8 (C1), 139.3 (C13), 117.6 (C2), 114.3 (C14), 35.4 (C15), 35.3 (C12), 33.9 (C5), 29.5 (C7), 29.5 (C8), 29.5 (C10), 29.2 (C9), 29.0 (C11), 25.5 (C6). HRMS (ESI,  $m/z$ ):  $[M + Na]^+$  calcd for  $C_{29}H_{47}N_3O_2$ , 492.3560; found, 492.3796.

DAP-M-Me-9 (**2c**):  $^1H$  NMR (400 MHz,  $CDCl_3$ ,  $\delta$ ): 7.74 (t,  $J = 7.9$  Hz, 1H, CH), 7.24 (d,  $J = 8.2$  Hz, 2H, CH), 5.99–5.61 (m, 2H, =CH), 5.10–4.81 (m, 4H, =CH<sub>2</sub>), 3.36 (s, 6H, CH<sub>3</sub>), 2.36 (t,  $J = 7.5$  Hz, 4H, CH<sub>2</sub>), 2.13–1.93 (m, 4H, CH<sub>2</sub>), 1.64 (t,  $J = 7.4$  Hz, 4H, CH<sub>2</sub>), 1.44–1.13 (m, 24H, CH<sub>2</sub>).  $^{13}C$  NMR (101 MHz,  $CDCl_3$ ,  $\delta$ ): 173.7 (C=O), 155.0 (C3), 139.8 (C1), 139.3 (C14), 117.6 (C2), 114.2 (C15), 35.4 (C16), 35.3 (C5), 33.9

(C13), 29.8 (C8), 29.5 (C7), 29.5 (C10), 29.5 (C11), 29.2 (C9), 29.1 (C12), 25.5 (C6). HRMS (ESI,  $m/z$ ):  $[M + Na]^+$  calcd for  $C_{31}H_{51}N_3O_2$ , 520.4893; found, 520.5265.

DAP-M-Bn-7 (**2d**):  $^1H$  NMR (400 MHz,  $CDCl_3$ ,  $\delta$ ): 7.61 (t,  $J = 7.9$  Hz, 1H, CH), 7.26–7.14 (m, 10H, CH), 7.10 (d,  $J = 7.6$  Hz, 2H, CH), 5.92–5.69 (m, 2H, =CH), 5.22–4.79 (m, 8H, =CH<sub>2</sub>), 2.24 (t,  $J = 7.3$  Hz, 4H, CH<sub>2</sub>), 2.06–1.91 (m, 4H, CH<sub>2</sub>), 1.67–1.53 (m, 4H, CH<sub>2</sub>), 1.38–1.13 (m, 16H, CH<sub>2</sub>).  $^{13}C$  NMR (101 MHz,  $CDCl_3$ ,  $\delta$ ): 173.6 (C=O), 154.1 (C3), 139.7 (C12), 139.2 (C1), 137.6 (C15), 128.6 (C17), 127.7 (C16), 127.3 (C18), 119.0 (C13), 114.3 (C2), 51.0 (C14), 35.3 (C5), 33.9 (C11), 29.4 (C7), 29.4 (C8), 29.1 (C10), 29.0 (C9), 25.4 (C6). HRMS (ESI,  $m/z$ ):  $[M + H]^+$  calcd for  $C_{39}H_{51}N_3O_2$ , 594.4054; found, 594.4369.

DAP-M-Bn-8 (**2e**):  $^1H$  NMR (400 MHz,  $CDCl_3$ ,  $\delta$ ): 7.61 (t,  $J = 7.9$  Hz, 1H, CH), 7.25–7.17 (m, 6H, CH), 7.15–7.04 (m, 6H, CH), 5.86–5.74 (m, 2H, =CH), 5.04–4.98 (m, 4H, CH<sub>2</sub>), 4.97–4.89 (m, 4H, =CH<sub>2</sub>), 2.24 (t,  $J = 7.4$  Hz, 4H, CH<sub>2</sub>), 2.02 (dd,  $J = 14.4$  Hz,  $J = 6.9$  Hz, 4H, CH<sub>2</sub>), 1.63–1.56 (m, 4H, CH<sub>2</sub>), 1.38–1.15 (m, 20H, CH<sub>2</sub>).  $^{13}C$  NMR (101 MHz,  $CDCl_3$ ,  $\delta$ ): 173.6 (C=O), 154.1 (C3), 139.7 (C13), 139.3 (C1), 137.6 (C16), 128.6 (C18), 127.7 (C19), 127.3 (C17), 119.0 (C2), 114.3 (C14), 51.0 (C15), 35.3 (C12), 33.9 (C5), 29.5 (C7), 29.4 (C8), 29.4 (C10), 29.2 (C9), 29.0 (C11), 25.5 (C6). HRMS (ESI,  $m/z$ ):  $[M + Na]^+$  calcd for  $C_{41}H_{55}N_3O_2$ , 644.4186; found, 644.4227.

DAP-M-Bn-9 (**2f**):  $^1H$  NMR (400 MHz,  $CDCl_3$ ,  $\delta$ ): 7.61 (t,  $J = 7.9$  Hz, 1H, CH), 7.25–7.15 (m, 10H, CH), 7.10 (dd,  $J = 7.7$  Hz,  $J = 1.9$  Hz, 2H, CH), 5.95–5.66 (m, 2H, =CH), 5.05–4.83 (m, 8H, =CH<sub>2</sub>), 2.24 (t,  $J = 7.5$  Hz, 4H, CH<sub>2</sub>), 2.11–1.92 (m, 4H, CH<sub>2</sub>), 1.69–1.50 (m, 4H, CH<sub>2</sub>), 1.45–1.12 (m, 24H, CH<sub>2</sub>).  $^{13}C$  NMR (101 MHz,  $CDCl_3$ ,  $\delta$ ): 173.6 (C=O), 154.1 (C3), 139.7 (C14), 139.3 (C1), 137.7 (C17), 128.6 (C19), 127.7 (C18), 127.3 (C20), 119.0 (C15), 114.3 (C2), 51.0 (C16), 35.3 (C5), 33.9 (C13), 29.6 (C9), 29.6 (C10), 29.5 (C8), 29.4 (C7), 29.3 (C12), 29.1 (C12), 25.5 (C6). HRMS (ESI,  $m/z$ ):  $[M + H]^+$  calcd for  $C_{43}H_{59}N_3O_2$ , 650.4680; found, 650.5027;  $[M + Na]^+$  calcd for  $C_{43}H_{59}N_3O_2$ , 672.4499; found, 672.4245.

### Synthesis of Undec-10-enamide

The synthesis was carried out analogous to literature.<sup>50</sup> A two-necked flask was filled with a  $NH_4OH$  solution (250 mL, 25% in  $H_2O$ ) and cooled to 0 °C. After dropwise addition of undec-10-enoyl chloride (47.70 mmol, 9.0 g), dissolved in THF (30 mL), the mixture was allowed to stir overnight. The final product was separated by filtration and dried in vacuum to yield 8.17 g (44.57 mmol, 93%) of a white solid. (**3**)  $^1H$  NMR (400 MHz,  $CDCl_3$ ,  $\delta$ ): 5.89–5.72 (m, 1H, =CH), 5.54 (d, 2H, NH<sub>2</sub>), 5.07–4.85 (m, 2H, =CH<sub>2</sub>), 2.25–2.17 (m, 2H, CH<sub>2</sub>), 2.10–1.98 (m, 2H, CH<sub>2</sub>), 1.71–1.55 (m, 2H, CH<sub>2</sub>), 1.45–1.17 (m, 10H, CH<sub>2</sub>).  $^{13}C$  NMR (101 MHz,  $CDCl_3$ ,  $\delta$ ): 175.9 (C=O), 139.3 (C10), 114.3 (C11), 36.1 (C2), 33.9 (C9), 29.4 (C5), 29.4 (C6), 29.4 (C7), 29.2 (C4), 29.0 (C8), 25.7 (C3). HRMS (ESI,  $m/z$ ):  $[M + Na]^+$  calcd for  $C_{11}H_{21}NO$ , 206.1515; found, 206.1449.

### Synthesis of Undec-10-en-1-amine

The synthesis was carried out according to the literature.<sup>50</sup> A two-necked flask was filled with undec-10-enamide (5.91 mmol, 1 g) dissolved in dry THF (30 mL). After cooling to  $-10\text{ }^{\circ}\text{C}$  and careful addition of  $\text{LiAlH}_4$  (8.86 mmol, 0.34 g), the mixture was allowed to stir overnight, followed by the addition of dry  $\text{Et}_2\text{O}$  (20 mL). By adding  $\text{H}_2\text{O}$  (1 mL) and then  $\text{NaOH}$  (2 mL, 10% in  $\text{H}_2\text{O}$ ) the reaction was quenched. Afterwards, the mixture was filtered and dried over  $\text{Na}_2\text{SO}_4$ . The solvent was removed in vacuum at  $45\text{ }^{\circ}\text{C}$  and the final product was obtained as a white waxy solid (5.06 mmol, 86%). (4)  $^1\text{H}$  NMR (400 MHz,  $\text{CDCl}_3$ ,  $\delta$ ): 5.89–5.71 (m, 1H, =CH), 5.04–4.86 (m, 2H, =CH<sub>2</sub>), 2.67 (t,  $J = 7.0$  Hz, 2H, CH<sub>2</sub>), 2.10–1.96 (m, 2H, CH<sub>2</sub>), 1.48–1.22 (m, 14H, CH<sub>2</sub>).  $^{13}\text{C}$  NMR (101 MHz,  $\text{CDCl}_3$ ,  $\delta$ ): 139.4 (C10), 114.2 (C11), 42.4 (C1), 34.0 (C9), 33.9 (C2), 29.7 (C4), 29.6 (C5), 29.6 (C6), 29.3 (C7), 29.1 (C8), 27.0 (C3). HRMS (ESI,  $m/z$ ):  $[M + \text{H}]^+$  calcd for  $\text{C}_{11}\text{H}_{23}\text{N}$ , 170.1903; found, 170.1907.

### Synthesis of 1,3-Diundec-10-en-1-ylurea

The synthesis was carried out according to the literature.<sup>53</sup> A one-necked flask was filled with undec-10-en-1-amine (4.99 mmol, 0.78 mg), ethylene carbonate (2.50 mmol, 0.22 mg), and 1,5,7-triazabicyclo[4.4.0]dec-5-ene (TBD) (0.05 mmol, 6.95 mg) and heated up to  $130\text{ }^{\circ}\text{C}$  for 2 h. After cooling the mixture to room temperature the crude product was purified via column chromatography (silica gel 60, DCM/EA 85:15) to yield 0.73 g of a pale yellow solid (1.99 mmol, 40%).

Urea-M-9 (5):  $^1\text{H}$  NMR (400 MHz,  $\text{CDCl}_3$ ,  $\delta$ ): 5.88–5.74 (m, 2H, =CH) 5.06–4.88 (m, 4H, =CH<sub>2</sub>), 4.23 (s, 2H, NH), 3.14 (t,  $J = 7.1$  Hz, 4H, CH<sub>2</sub>), 2.12–1.96 (m, 4H, CH<sub>2</sub>), 1.48 (t,  $J = 7.0$  Hz, 4H, CH<sub>2</sub>) 1.40–1.24 (m, 24H, CH<sub>2</sub>).  $^{13}\text{C}$  NMR (101 MHz,  $\text{CDCl}_3$ ,  $\delta$ ): 158.3 (C=O), 139.3 (C11), 114.3 (C12), 40.9 (C2), 33.9 (C10), 30.4 (C3), 29.7 (C8), 29.6 (C7), 29.5 (C5), 29.3 (C6), 29.1 (C9), 27.1 (C4). HRMS (ESI,  $m/z$ ):  $[M + \text{Na}]^+$  calcd for  $\text{C}_{23}\text{H}_{44}\text{N}_2\text{O}$ , 387.3346; found, 387.3049;  $[M + \text{H}]^+$  calcd for  $\text{C}_{23}\text{H}_{44}\text{N}_2\text{O}$ , 365.3526; found, 365.3292.

### Polymerization

The polymerizations were carried out under an atmosphere of nitrogen as bulk polymerization.<sup>54</sup> A Schlenk tube was filled with the monomers (1a–c, 2a–f or 5) and the appropriate amount of Grubbs' 1st generation catalyst (250:1 monomer to catalyst ratio) was transferred to the Schlenk tube under a counterflow of nitrogen. The reaction mixture was heated up to  $65\text{ }^{\circ}\text{C}$  in case of the protected monomers (2a–f) or up to  $130\text{ }^{\circ}\text{C}$  in case of the unprotected monomers (1a–f, 5), followed by the application of vacuum ( $p \sim 3$  mbar) to remove the generated ethylene. After the evolution of ethylene stopped and the magnetic stir bar was unable to move due to the increased viscosity the polymerization was quenched by opening the Schlenk tube. The crude polymer was dissolved in a small amount of THF and precipitated into cold methanol to remove unreacted monomer and residual catalyst and was obtained as white to beige solid in yields ranging from 73 to 97%. Polymers 6a–c and 8 could

not be analyzed by the means of NMR spectroscopy or MALDI-ToF MS due to their insolubility in any tested solvent.

DAP-uP-Me-16 (6d):  $^1\text{H}$  NMR (400 MHz,  $\text{CDCl}_3$ ,  $\delta$ ): 7.75 (t,  $J = 7.9$  Hz, 1H, CH), 7.23 (bs, 2H, CH), 5.88–5.69 (m, 2H, =CH), 5.43–5.26 (m, 2H, =CH), 5.04–4.86 (m, 4H, =CH<sub>2</sub>), 3.36 (s, 6H, CH<sub>3</sub>), 2.36 (t,  $J = 7.5$  Hz, 4H, CH<sub>2</sub>), 2.05–1.87 (m, 8H, CH<sub>2</sub>), 1.75–1.52 (m, 4H, CH<sub>2</sub>), 1.38–1.13 (m, 28H, CH<sub>2</sub>).  $^{13}\text{C}$  NMR (126 MHz,  $\text{CDCl}_3$ ,  $\delta$ ): 173.7 (C=O), 154.9 (C3), 139.8 (C1), 130.4 (C12), 117.6 (C2), 35.4 (C13), 35.3 (C5), 32.7 (C11), 29.9 (C7), 29.8 (C10), 29.5 (C8), 29.5 (C14), 29.3 (C9), 29.2 (C16), 27.3 (C15), 25.5 (C6).

DAP-uP-Me-18 (6e):  $^1\text{H}$  NMR (400 MHz,  $\text{CDCl}_3$ ,  $\delta$ ): 7.75 (t,  $J = 7.9$  Hz, 1H, CH), 7.26 (bs, 2H, CH), 5.91–5.71 (m, 2H, =CH), 5.45–5.20 (m, 2H, =CH), 5.07–4.73 (m, 4H, =CH<sub>2</sub>), 3.36 (s, 6H, CH<sub>3</sub>), 2.36 (t,  $J = 7.5$  Hz, 4H, CH<sub>2</sub>), 2.07–1.85 (m, 4H, CH<sub>2</sub>), 1.73–1.52 (m, 8H, CH<sub>2</sub>), 1.24 (bs, 28H, CH<sub>2</sub>).  $^{13}\text{C}$  NMR (101 MHz,  $\text{CDCl}_3$ ,  $\delta$ ): 173.7 (C=O), 154.9 (C3), 139.8 (C1), 139.3 (C18), 130.4 (C13), 117.7 (C2), 114.3 (C19), 35.4 (C14), 35.3 (C5), 33.9 (C17), 32.7 (C12), 29.9 (C8), 29.8 (C7), 29.6 (C11), 29.5 (C15), 29.5 (C16), 29.3 (C10), 29.2 (C9), 25.5 (C6).

DAP-uP-Me-20 (6f):  $^1\text{H}$  NMR (500 MHz,  $\text{CDCl}_3$ ,  $\delta$ ): 7.75 (t,  $J = 7.9$  Hz, 1H, CH), 7.24 (d,  $J = 3.9$  Hz, 2H, CH), 5.88–5.64 (m, 2H, =CH), 5.47–5.12 (m, 2H, =CH), 5.07 – 4.78 (m, 4H, =CH<sub>2</sub>), 3.36 (s, 6H, CH<sub>3</sub>), 2.36 (t,  $J = 7.5$  Hz, 4H, CH<sub>2</sub>), 2.08–1.84 (m, 8H, CH<sub>2</sub>), 1.71–1.48 (m, 4H, CH<sub>2</sub>), 1.40–1.04 (m, 32H, CH<sub>2</sub>).  $^{13}\text{C}$  NMR (126 MHz,  $\text{CDCl}_3$ ,  $\delta$ ): 173.7 (C=O), 155.0 (C3), 139.8 (C1), 139.3 (C19), 130.5 (C14), 117.7 (C2), 114.3 (C20), 35.4 (C15), 35.3 (C5), 33.9 (C18), 32.8 (C13), 29.9 (C10), 29.8 (C8), 29.6 (C7), 29.6 (C12), 29.6 (C16), 29.5 (C11), 29.5 (C9), 29.3 (C17), 25.5 (C6).

DAP-uP-Bn-16 (6g):  $^1\text{H}$  NMR (400 MHz,  $\text{CDCl}_3$ ,  $\delta$ ): 7.60 (t,  $J = 7.9$  Hz, 1H, CH), 7.24–7.14 (m, 10H, CH), 7.14–6.99 (m, 2H, CH), 5.89–5.71 (m, 2H, =CH), 5.41–5.26 (m, 2H, =CH), 5.01 (s, 4H, CH<sub>2</sub>) 4.98–4.85 (m, 4H, =CH<sub>2</sub>), 2.35–2.15 (m, 4H, CH<sub>2</sub>), 2.06–1.86 (m, 8H, CH<sub>2</sub>), 1.69–1.51 (m, 4H, CH<sub>2</sub>), 1.38–1.12 (m, 28H, CH<sub>2</sub>).  $^{13}\text{C}$  NMR (126 MHz,  $\text{CDCl}_3$ ,  $\delta$ ): 173.6 (C=O), 154.1 (C3), 139.7 (C22), 137.7 (C1), 130.4 (C14), 130.0 (C12), 128.6 (C16), 127.7 (C15), 127.3 (C17), 119.0 (C2), 114.3 (C23), 51.0 (C13), 35.3 (C5), 32.7 (C21), 29.9 (C11), 29.8 (C7), 29.5 (C10), 29.4 (C8), 29.4 (C18), 29.3 (C9), 29.2 (C20), 29.1 (C19), 25.5 (C6).

DAP-uP-Bn-18 (6h):  $^1\text{H}$  NMR (500 MHz,  $\text{CDCl}_3$ ,  $\delta$ ): 7.60 (t,  $J = 7.9$  Hz, 1H, CH), 7.24–7.14 (m, 10H, CH), 7.10 (d,  $J = 6.7$  Hz, 2H, CH), 5.87–5.72 (m, 2H, =CH), 5.42–5.27 (m, 2H, =CH), 5.08–4.86 (m, 8H, =CH<sub>2</sub>), 2.23 (t,  $J = 7.0$  Hz, 4H, CH<sub>2</sub>), 2.04–1.88 (m, 8H, CH<sub>2</sub>), 1.68–1.52 (m, 4H, CH<sub>2</sub>), 1.37–1.10 (m, 28H, CH<sub>2</sub>).  $^{13}\text{C}$  NMR (126 MHz,  $\text{CDCl}_3$ ,  $\delta$ ): 173.6 (C=O), 154.1 (C3), 139.8 (C22), 137.7 (C1), 130.5 (C13), 130.0 (C17), 128.6 (C16), 127.3 (C18), 119.0 (C2), 50.9 (C14), 35.3 (C5), 32.8 (C12), 29.9 (C8), 29.8 (C7), 29.6 (C11), 29.5 (C9\*), 29.5 (C19), 29.5 (C20), 29.3 (C10), 29.2 (C9), 27.4 (C6).

DAP-uP-Bn-20 (6i):  $^1\text{H}$  NMR (500 MHz,  $\text{CDCl}_3$ ,  $\delta$ ): 7.60 (t,  $J = 7.9$  Hz, 1H, CH), 7.24–7.16 (m, 10H, CH), 7.10 (d,  $J = 6.5$

Hz, 2H, CH), 5.91–5.68 (m, 2H, =CH), 5.46–5.21 (m, 2H, =CH), 5.10–4.79 (m, 4H, =CH<sub>2</sub>), 2.23 (t,  $J = 7.0$  Hz, 4H, CH<sub>2</sub>), 2.07–1.88 (m, 8H, CH<sub>2</sub>), 1.70–1.43 (m, 4H, CH<sub>2</sub>), 1.38–1.11 (m, 32H, CH<sub>2</sub>). <sup>13</sup>C NMR (126 MHz, CDCl<sub>3</sub>,  $\delta$ ): 173.6 (C=O), 154.1 (C3), 139.7 (C23), 137.7 (C1), 130.5 (C16), 130.0 (C14), 128.6 (C18), 127.7 (C17), 127.3 (C19), 119.0 (C2), 51.0 (C15), 35.3 (C5), 33.9 (C22), 32.8 (C13), 29.9 (C10), 29.8 (C7), 29.6 (C8), 29.6 (C12), 29.6 (C20), 29.5 (C11), 29.4 (C9), 29.4 (C21), 25.5 (C6).

### Hydrogenation

A one-necked flask was filled with the appropriate polymer **6a–i** or **8** (1 eq.), *p*-toulenesulfonylhydrazide (TsNHNH<sub>2</sub>) (4 eq. according to the amount of double bonds), *N,N*-diisopropylethylamine (2.7 eq.), and *N,N*-dimethylformamide (DMF) (10 mL). The reaction mixture was flushed with nitrogen for 30 min and was heated to 150 °C for 6 h under vigorous stirring. After cooling to room temperature the solvent was removed in vacuum at 45 °C, followed by the addition of THF in order to dissolve the crude product. The final polymer was obtained by precipitation into cold methanol as a beige solid in yields ranging from 68 to 94%.

DAP-sP-Me-16 (**7d**): <sup>1</sup>H NMR (500 MHz, CDCl<sub>3</sub>,  $\delta$ ): 7.75 (t,  $J = 7.9$  Hz, 1H, CH), 7.24 (d,  $J = 5.6$  Hz, 2H, CH), 3.36 (s, 6H, CH<sub>3</sub>), 2.36 (t,  $J = 7.5$  Hz, 4H, CH<sub>2</sub>), 1.70–1.51 (m, 4H, CH<sub>2</sub>), 1.34–1.13 (m, 36H, CH<sub>2</sub>), 0.96–0.75 (m, 6H, CH<sub>3</sub>). <sup>13</sup>C NMR (126 MHz, CDCl<sub>3</sub>,  $\delta$ ): 173.8 (C=O), 155.0 (C3), 139.8 (C1), 117.7 (C2), 35.4 (C12), 35.3 (C5), 32.0 (C14), 29.8 (C8), 29.8 (C7), 29.8 (C10), 29.7 (C11), 29.6 (C13), 29.5 (C9), 25.5 (C6), 22.8 (C15), 14.3 (C16).

DAP-sP-Me-18 (**7e**): <sup>1</sup>H NMR (400 MHz, CDCl<sub>3</sub>,  $\delta$ ): 7.75 (t,  $J = 7.8$  Hz, 1H, CH), 7.24 (d,  $J = 7.1$  Hz, 2H, CH), 3.36 (s, 6H, CH<sub>3</sub>), 2.35 (t,  $J = 7.5$  Hz, 4H, CH<sub>2</sub>), 1.72–1.53 (m, 4H, CH<sub>2</sub>), 1.23 (bs, 40H, CH<sub>2</sub>), 0.86 (t, 6H,  $J = 6.7$  Hz). <sup>13</sup>C NMR (101 MHz, CDCl<sub>3</sub>,  $\delta$ ): 173.7 (C=O), 155.0 (C3), 139.8 (C1), 117.7 (C2), 35.4 (C12), 35.3 (C5), 32.0 (C14), 29.8 (C8), 29.8 (C7), 29.8 (C10), 29.7 (C11), 29.6 (C13), 29.5 (C9), 25.5 (C6), 22.8 (C15), 14.2 (C16).

DAP-sP-Me-20 (**7f**): <sup>1</sup>H NMR (400 MHz, CDCl<sub>3</sub>,  $\delta$ ): 7.75 (t,  $J = 8.0$  Hz, 1H, CH), 7.24 (d,  $J = 8.4$  Hz, 2H, CH), 3.36 (s, 6H, CH<sub>3</sub>), 2.39–2.32 (m, 4H, CH<sub>2</sub>), 1.68–1.58 (m, 4H, CH<sub>2</sub>), 1.32–1.15 (m, 48H, CH<sub>2</sub>), 0.87 (t,  $J = 6.8$  Hz, 6H, CH<sub>3</sub>). <sup>13</sup>C NMR (101 MHz, CDCl<sub>3</sub>,  $\delta$ ): 173.7 (C=O), 155.0 (C3), 139.8 (C1), 117.7 (C2), 35.4 (C12), 35.3 (C5), 32.1 (C15), 29.9 (C8), 29.9 (C7), 29.8 (C10), 29.8 (C11), 29.7 (C13), 29.6 (C14), 29.5 (C9), 25.5 (C6), 22.8 (C16), 14.3 (C17).

DAP-sP-Bn-16 (**7g**): <sup>1</sup>H NMR (400 MHz, CDCl<sub>3</sub>,  $\delta$ ): 7.60 (t,  $J = 7.9$  Hz, 1H, CH), 7.24–7.12 (m, 10H, CH), 7.09 (d,  $J = 6.5$  Hz, 2H, CH), 5.01 (s, 4H, CH<sub>2</sub>), 2.23 (t,  $J = 7.1$  Hz, 4H, CH<sub>2</sub>), 1.66–1.49 (m, 4H, CH<sub>2</sub>), 1.21 (bs, 40H, CH<sub>2</sub>), 0.86 (t,  $J = 6.8$  Hz, CH<sub>3</sub>). <sup>13</sup>C NMR (101 MHz, CDCl<sub>3</sub>,  $\delta$ ): 173.6 (C=O), 154.1 (C3), 139.8 (C1), 137.7 (C13), 128.6 (C15), 127.7 (C14), 127.3 (C16), 119.0 (C2), 51.0 (C12), 35.3 (C5), 29.8 (C8), 29.8 (C7), 29.7 (C10), 29.6 (C11), 29.5 (C9), 25.5 (C6), 21.2 (C19).

DAP-sP-Bn-18 (**7h**): <sup>1</sup>H NMR (400 MHz, CDCl<sub>3</sub>,  $\delta$ ): 7.60 (t,  $J = 7.9$  Hz, 1H, CH), 7.24–7.14 (m, 10H, CH), 7.10 (d,  $J = 6.3$  Hz, 2H, CH), 5.01 (s, 4H, CH<sub>2</sub>), 2.23 (t,  $J = 7.2$  Hz, 4H, CH<sub>2</sub>), 1.66–1.50 (m, 4H, CH<sub>2</sub>), 1.44–1.06 (m, 40H, CH<sub>2</sub>), 0.95–0.77 (m, 6H). <sup>13</sup>C NMR (101 MHz, CDCl<sub>3</sub>,  $\delta$ ): 173.6 (C=O), 154.1 (C3), 139.7 (C1), 137.7 (C13), 128.6 (C15), 127.7 (C14), 127.3 (C16), 119.0 (C2), 51.0 (C12), 35.3 (C5), 29.9 (C8), 29.9 (C7), 29.8 (C10), 29.7 (C11), 29.6 (C17), 29.5 (C9), 25.5 (C6).

DAP-sP-Bn-20 (**7i**): <sup>1</sup>H NMR (500 MHz, CDCl<sub>3</sub>,  $\delta$ ): 7.60 (t,  $J = 7.9$  Hz, 1H, CH), 7.25–7.15 (m, 10H, CH), 7.14–6.98 (m, 2H, CH), 5.01 (s, 4H, CH<sub>2</sub>), 2.23 (t,  $J = 7.2$  Hz, 4H, CH<sub>2</sub>), 1.64–1.49 (m, 4H, CH<sub>2</sub>), 1.34–1.09 (m, 48H, CH<sub>2</sub>), 0.92–0.76 (m, 6H, CH<sub>3</sub>). <sup>13</sup>C NMR (126 MHz, CDCl<sub>3</sub>,  $\delta$ ): 173.6 (C=O), 154.1 (C3), 139.7 (C1), 137.7 (C13), 128.6 (C15), 127.7 (C14), 127.3 (C16), 119.0 (C2), 51.0 (C12), 35.3 (C5), 29.9 (C19), 29.9 (C8), 29.9 (C7), 29.8 (C10), 29.7 (C11), 29.6 (C17), 29.5 (C18), 29.4 (C9), 25.5 (C6), 21.0 (C20), 14.3 (C21).

## RESULTS AND DISCUSSION

ADMET polymerization and subsequent hydrogenation were used to synthesize various precision polymers (**7a–i** and **9**) bearing the different functional groups (DAP and urea) along the polymer backbone. DAP and urea moieties were incorporated into the polyethylene backbone via specially designed symmetrical monomers. These planar groups are able to act as fold-inducing element on the polymer chain due to their conformation and are able to interact via supramolecular interactions ( $\pi$ - $\pi$ -stacking and hydrogen bonding), thus influencing the final crystalline morphology. By variation of the alkyl chain length of the monomer the position of the functional group in the polymer backbone can be determined precisely, whereby precision polymers bearing this defect after every 16th, 18th, or 20th carbon were obtained. In this article, we are examining the effect of different supramolecular interactions between adjacent polymer chains on the chain packing and crystallization of precision polymers.

### Monomer Synthesis

The required monomers **1a–c**, **2a–f**, and **5** bearing a DAP unit were synthesized as mentioned previously<sup>51</sup> in a Schotten-Baumann reaction using DCM and water as solvent and NaOH as base, whereby acid chlorides with different alkyl chain lengths ( $x = 7, 8, 9$ ) and DAP were chosen as precursors. Subsequently, the free amide groups were protected by the reaction of the unprotected monomers **1a–c** with either methyl iodide or benzyl bromide to sustain the solubility of the compounds after polymerization (see Scheme 1). All DAP monomers (**1a–f**, **2a–f**) were analyzed via <sup>1</sup>H and <sup>13</sup>C NMR spectroscopy as well as ESI-ToF MS and the corresponding spectra are shown in Supporting Information Figures S1–S9. The assignment of all resonances was possible and confirmed the purity of all compounds. The synthesis of monomer **5**, bearing a urea group, was accomplished in the first step by the reaction of undec-9-enoyl chloride with

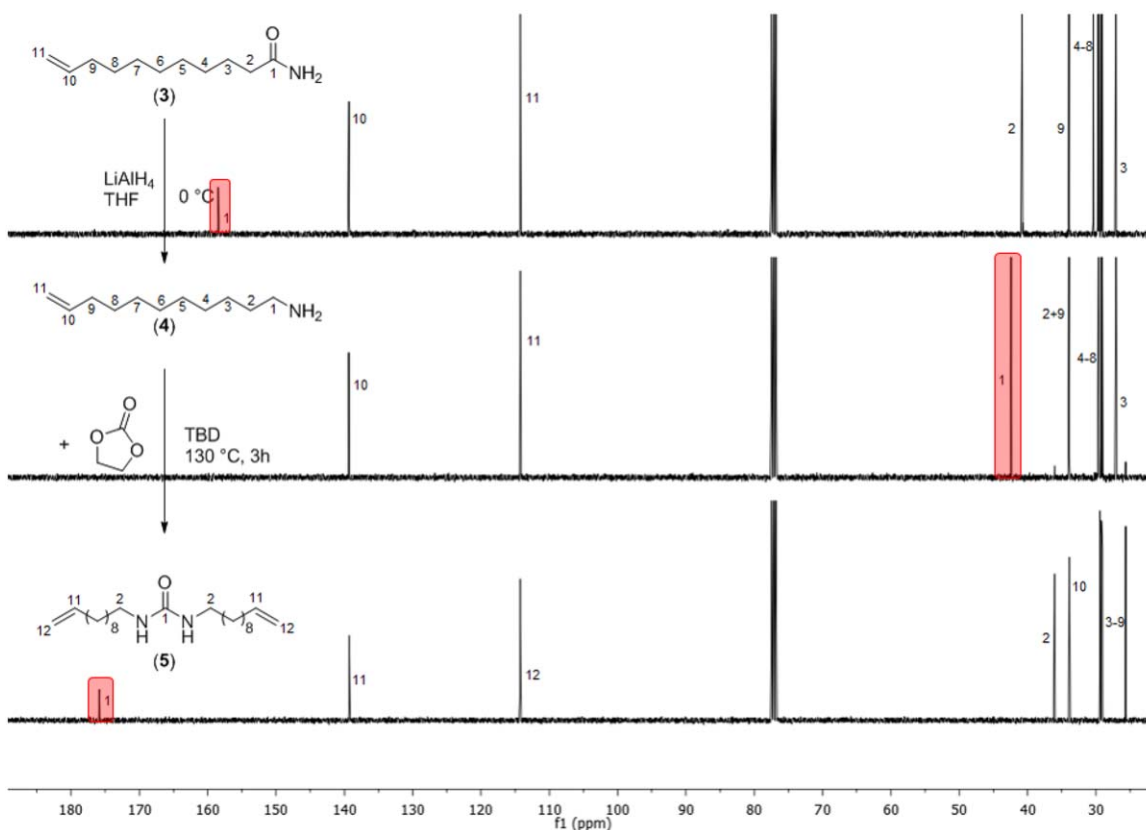


**FIGURE 1**  $^{13}\text{C}$  NMR spectra of undec-10-enamide (**3**) (top), undec-10-en-1-amine (**4**) (middle), and 1,3-diundec-10-en-1-ylurea (**5**) (bottom). [Color figure can be viewed at [wileyonlinelibrary.com](http://wileyonlinelibrary.com)]

ammonium hydroxide yielding undec-10-enamide (**3**) as a white solid. Successful conversion was proven by the shift of the signal assigned to the carbonyl group from 174.1 ppm to 175.9 ppm as well as the shift of signal belonging to the adjacent  $\text{CH}_2$  group from 46.9 ppm to 36.1 ppm in the  $^{13}\text{C}$  NMR spectrum as shown in Figure 1 (top). Via subsequent reduction of compound **3** with  $\text{LiAlH}_4$  in dry THF at  $0^\circ\text{C}$  undec-10-en-1-amine (**4**) could be obtained, resulting in the disappearance of the signal of the carbonyl group in the  $^{13}\text{C}$  NMR spectrum (Fig. 1 middle). In a final step this amine was then reacted with ethylene carbonate under use of 1,5,7-triazabicyclo[4.4.0]dec-5-ene (TBD) as organocatalyst without any solvents at  $130^\circ\text{C}$ . The purity of the obtained precursors (**3** and **4**) as well as the urea-monomer (**5**) was proven via  $^1\text{H}$  and  $^{13}\text{C}$  NMR spectroscopy as well as ESI-ToF MS (see Supporting Information Figs. S10–S14). All resonances can clearly be assigned and especially the carbonyl function (158.5 ppm) and the allylic carbons (139.3 and 114.3 ppm) shown in Figure 1 (bottom) prove the complete conversion into the symmetrical urea. The reaction scheme for the monomer syntheses as well as the polymerization and subsequent hydrogenation is shown in Scheme 1.

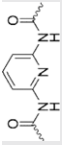
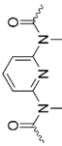
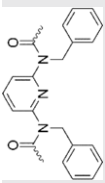
### Polymerization

All polymerizations were carried out as bulk polymerizations as the used monomers (**1a–c**, **2a–f**, and **5**) are either viscous liquids or present in the molten state at the chosen

polymerization temperature.<sup>54</sup> Grubbs' 1st generation catalyst has been demonstrated as an advantageous catalyst for ADMET due to its relatively high stability and low isomerization rate. Although, the reaction was not quenched with ethyl vinyl ether as usual<sup>55</sup> both NMR analysis and MALDI ToF MS showed that no residual catalyst, neither attached to the polymer chain nor as impurity, was present. The successful conversion can be proven by the occurrence of the olefinic signals in the  $^1\text{H}$  and  $^{13}\text{C}$  NMR spectra in the range of 5.31–5.38 ppm and 130 ppm, respectively (see Supporting Information Figs. S15–S18), which can be assigned to the newly developed internal double bonds.<sup>30,56,57</sup>

The obtained molecular weights and associated polydispersity indices are listed in Table 1. The polymers without protection group (**6a–c** and **8**) could not be characterized by SEC and NMR spectroscopy due to their insolubility in any tested solvent presumably caused by the formation of hydrogen bonds and the segregation from the saturated alkyl chains. Therefore, in these cases (polymers **6a–c** and **8**) the progress of polymerization was monitored via IR spectroscopy, monitoring the characteristic absorption bands of the monomers (**1c** and **5**) at  $\sim 911$  and  $\sim 991\text{ cm}^{-1}$ , which represent the C–H out-of-plane deformation vibration of the vinylic end groups. After polymerization the intensities of these bands are decreased and a new band at  $\sim 963\text{ cm}^{-1}$  becomes apparent, which is related to C–H out-of-plane

**TABLE 1** Molecular Weights and Thermal Properties of the Synthesized DAP (**6a–i**, **7a–i**) and Urea Polymers (**8**, **9**)

Functional Group	Polymer	$M_n^a$ (g mol <sup>-1</sup> )	$M_n^b$ (g mol <sup>-1</sup> )	PDI	$T_g$ (°C)	$T_m$ (°C)	$T_c$ (°C)	$\Delta H_m$ (J g <sup>-1</sup> )	$\Delta T$ (°C)	$X_c$ (%)
	<b>6a</b>	c	c	–	–	123.3	108.3	59.99	15.0	27
	<b>6b</b>	–	–	–	–	137.7	118.7	53.94	19.0	23
	<b>6c</b>	–	–	–	–	123.3	95.9	47.99	27.4	19
	<b>7a</b>	–	–	–	–	167.7	139.7	73.06	28.0	32
	<b>7b</b>	–	–	–	–	167.8	138.8	55.20	29.0	24
	<b>7c</b>	–	–	–	–	154.8	128.7	57.07	26.1	23
	<b>6d</b>	4250	20,520	1.6	-16.8	–	–	–	–	–
	<b>6e</b>	3640	4970	1.5	–	57.1	–	36.05	–	21
	<b>6f</b>	8980	9200	1.8	–	62.3	-7.3	32.90	69.6	17
	<b>7d</b>	3880	2272	1.4	–	89.2	38.6	73.70	50.6	33
	<b>7e</b>	4320	2800	1.3	–	86.2	41.3	80.57	44.9	35
	<b>7f</b>	6380	8310	1.8	–	96.3	63.6	45.68	32.7	18
	<b>6g</b>	2720	7680	2.2	-7.7	–	–	–	–	–
	<b>6h</b>	4370	29,850	2.1	-10.1	–	–	–	–	–
	<b>6i</b>	9890	20,510	2.1	-8.6	–	–	–	–	–
	<b>7g</b>	4430	8200	1.6	-8	–	–	–	–	–
	<b>7h</b>	7460	8630	1.4	-2.2	–	–	–	–	–
	<b>7i</b>	10,000	9930	1.9	–	15.0	9.3	28.83	5.7	12
	<b>8</b>	c	c	–	–	116.0	85.0	32.44	31.0	13
	<b>9</b>	–	–	–	–	125.0	94.6	58.81	30.4	24

<sup>a</sup> Determined by SEC analysis in THF using polystyrene calibration.

<sup>b</sup> Determined by NMR analysis.

<sup>c</sup> Determination of the molecular weight and the molecular weight distribution was not possible due to insolubility of the samples.

vibration of the newly formed internal C=C double bonds<sup>18</sup> (see the corresponding IR spectra in Figure 2 and Supporting Information Fig. S19).

### Hydrogenation

The hydrogenation of the polymers was achieved by the reaction with TsNHNH<sub>2</sub> and *N,N*-diisopropylethylamine in DMF at 150 °C for 6h, which already turned out to be a successful method,<sup>51,57–59</sup> proving the completeness to the fully saturated polymers (**7d–i**) by the disappearance of all olefinic signals (from 4.90 to 5.84 ppm) and the formation of

terminal methyl groups (0.85–0.88 ppm) in the <sup>1</sup>H NMR spectra (see Supporting Information Fig. S20). The unsaturated polymers without protection groups (**6a–c** and **8**) were subjected to the same method, proving completion of the hydrogenation of the polymers **6a–c** and **8** via IR spectroscopy by the disappearance of the absorption band at ~963 cm<sup>-1</sup> (see Fig. 2 and Supporting Information Fig. S19). All DAP polymers with methyl protection group (**6d–f** and **7d–f**) were also characterized by MALDI-ToF MS and the corresponding spectra are shown in Figure 3 as well as Supporting Information Figures S21 and S22.

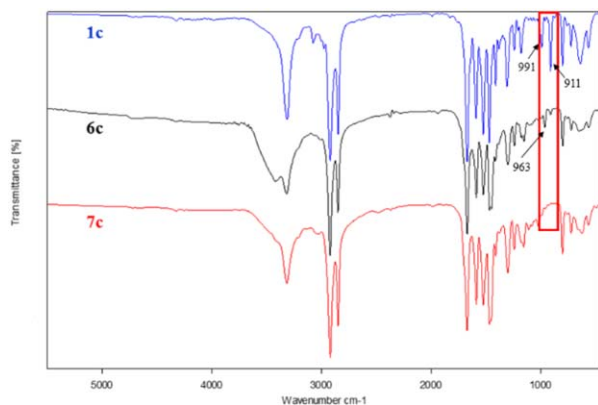


**FIGURE 2** Infrared spectra of the unprotected DAP monomer (**1c**) as well as the resulting unsaturated (**6c**) and saturated (**7c**) polymer. [Color figure can be viewed at wileyonlinelibrary.com]

All polymers show a mass distribution from 1200 to 7000 g mol<sup>-1</sup>. One to three different series can be assigned, whereby the main series always shows our linear polymers (**6d–f**, **7d–f**) as Li adducts. The other series indicate the fragmentation of our polymers due to the relatively high laser energy required for desorption during the MALDI process. The distance between two peaks of each series accounts for ~413 g mol<sup>-1</sup> to ~471 g mol<sup>-1</sup>, which is indicative for the corresponding repetitive DAP unit containing 16 to 20 alk(en)yl units.

### Thermal Analysis

The thermal behavior of all synthesized polymers was determined via DSC measurements. Selected heating curves, derived from the second heating run, are shown in Figure 4.

All benzyl protected polymers (**6g–i** and **7g,h**), except **7i** are amorphous, showing no melting point but only a glass

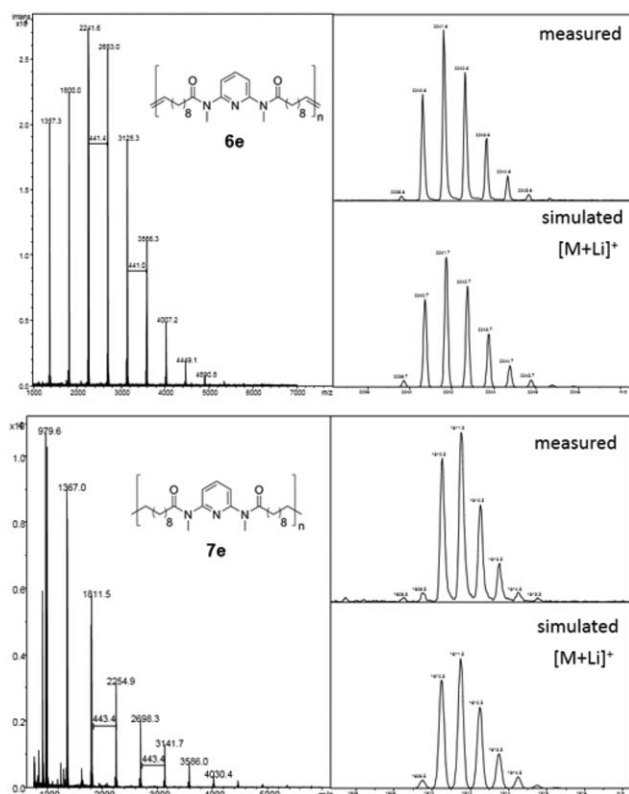


**FIGURE 3** MALDI-ToF mass spectra of the non-hydrogenated (**6e**) and hydrogenated (**7e**) DAP-polymers with methyl protection group and a methylene spacer length of  $n = 18$ .

transition in the range of  $-10$  to  $-2$  °C (Supporting Information Fig. S23). Only the fully hydrogenated polymer with the longest methylene spacer length (**7i**, solid green curve) shows a small endotherm in the heating curve indicating a 12% crystallinity and a melting temperature of 15 °C, explainable by the size of the benzyl protection group, which is too big to be incorporated into the crystal and thus hinders crystallization, compensated only by an increasing chain length of the alkyl chain in between the functional groups, in

turn enabling the formation of alkyl-crystals.<sup>57</sup> If an *N*-methyl protection group is used instead, only the unsaturated polymer with the shortest methylene spacer length (**6d**) shows no crystallinity, whereas all of the other methyl protected polymers (**6e–f**) show crystallinities in the range of 17–35%. Removing the methyl protection group (polymers **6a–c**) leads to an increase in melting temperature from 123 up to 138 °C, certainly by the hydrogen bonding between the DAP units, thus enhancing the thermal stability of this polymers. A similar behavior was also observed for diketopiperazine (DKP) functionalized polyethylenes, also capable of hydrogen bonding.<sup>55</sup> A significant structural difference between these DKP and our DAP polymers lies in the substitution position of the defects. Thus, the *para*-substituted DKP moieties can be included more easily into the all-*trans* PE-chain compared to our *meta*-substituted DAP moieties. This leads, in combination with the higher number of H-bonds between adjacent polymer chains (DKP = 4 H-bonds, DAP = 2 H-bonds), to higher melting points. The polymer bearing a urea group (**8**) also shows melting at elevated temperatures ( $T_m = 116$  °C), explained by supramolecular interactions between adjacent functional groups. Hydrogenation of the samples (polymers **7a–f**, **9**) leads to an increase in melting temperatures of about 30 °C and slightly increased crystallinities compared to the non-hydrogenated polymers **6a–f** and **8** [see Fig. 4(b)].

The unprotected DAP-polymers (**7a–c**) exhibit melting temperatures, that are above the  $T_m$  of pure ADMET polyethylene ( $T_m = 134$  °C),<sup>39</sup> explainable by enhanced thermal stability due to hydrogen bonds, comparable to polymers bearing sulfone groups along the polyethylene backbone as demonstrated in literature.<sup>30</sup> The observed cold crystallization apparent in every melting endotherm of the protected DAP polymers (**6d–f** and **7d–f**) can be interpreted as an at least partial incorporation of the functional group into the crystalline lamella, as the additional high supercooling ( $\Delta T = 32$ – $69$  °C) implies a slower crystallization rate, similar to observations for other precision polymers.<sup>37,44,58</sup> Supercooling decreases for the DAP polymers without protection

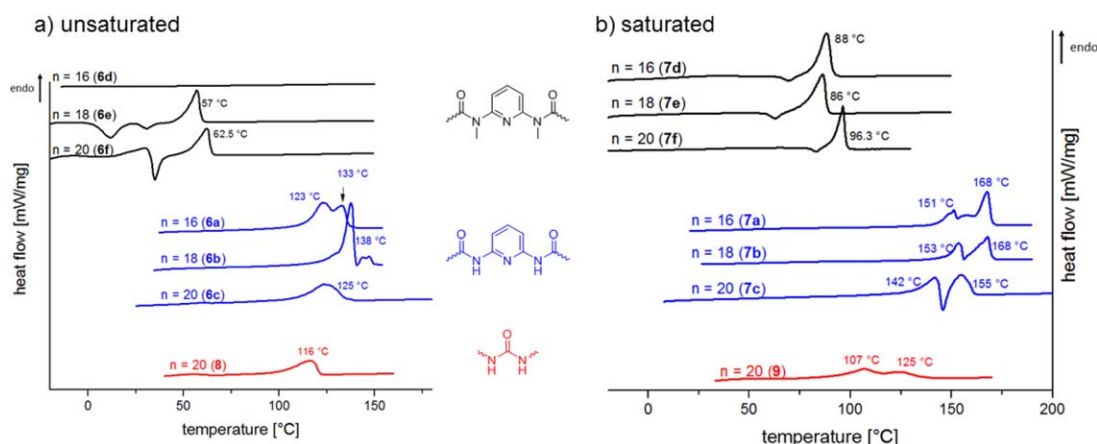


**FIGURE 4** DSC heating curves (second heating run) of the (a) unsaturated polymers (**6a–f** and **8**) and the (b) saturated polymers (**7a–f** and **9**). [Color figure can be viewed at [wileyonlinelibrary.com](http://wileyonlinelibrary.com)]

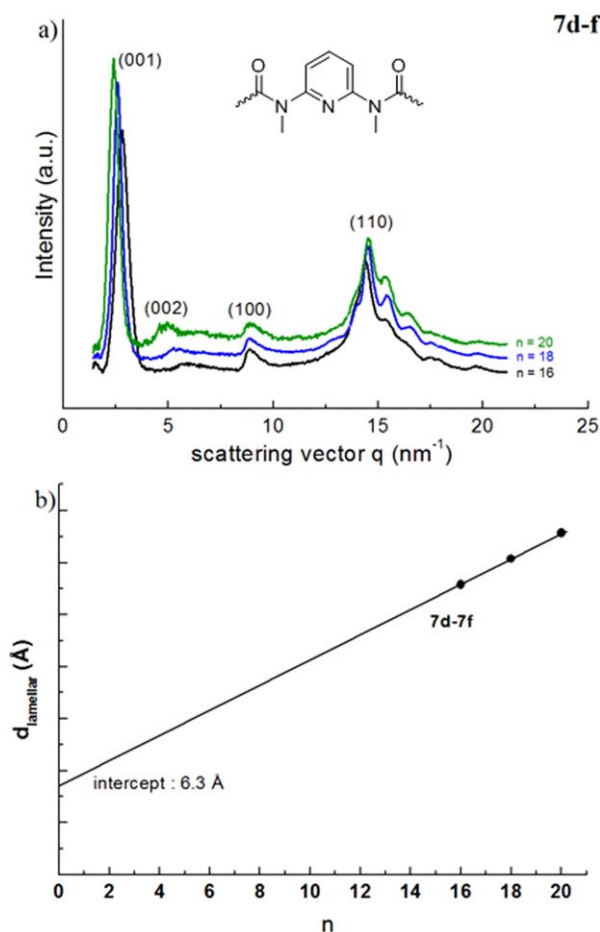


**FIGURE 5** (a) X-ray diffraction patterns of the saturated DAP polymers with methyl protection group and varying methylene spacer lengths (**7d–f**). (b) Plot of lamellar spacing  $d_{001}$  calculated based on Bragg's law as a function of methylene spacer length. [Color figure can be viewed at [wileyonlinelibrary.com](http://wileyonlinelibrary.com)]

group **7a–c** ( $\Delta T = 15\text{--}30\text{ }^\circ\text{C}$ ) as well as for the polymer bearing a urea group **9** ( $\Delta T = 31\text{ }^\circ\text{C}$ ), indicating the facilitated inclusion of the defects into the crystalline lamella. In the heating curves of the saturated polymers **7a–c** and **9** predominantly two melting endotherms (in the case of **7c** even a melting-recrystallization) are visible, suggestive of the formation of different polymorphs, similar to observations of polyethylene bearing a *para*-phenylene ether group along the polymer backbone.<sup>58</sup> All thermal data are listed in Table 1.

## Structural Analysis

### Protected DAP Polymers (**7d–f**)

Structural details of a series of saturated DAP polymers with methyl protection group and varying number of methylene units ( $n = 16, 18, \text{ and } 20$ ) (**7d–f**) in the methylene spacer are initially studied as representative example by wide angle X-ray diffraction (WAXD). The experiments are aimed to understand the influence of different spacer lengths and different chemical entities on the overall crystalline state [Fig. 5(a)].

Characteristic for all samples is a (001) reflection in the range  $2.4 < q < 2.8\text{ nm}^{-1}$ , corresponding to lattice planes indicating the distance between two DAP-units along the chain. The presence of a higher order reflection (002) at  $4.8 < q < 5.6\text{ nm}^{-1}$  indicates a lamellar morphology, also observed for precision sulfone polyethylenes.<sup>30</sup> The (001) reflection as well as the second order peak (002) shifts systematically to higher  $q$  values (corresponding to lower distances according to Bragg's law  $d_{hkl} = 2\pi/q_{hkl}$ ) with decreasing methylene spacer length. All diffraction patterns show a signal at  $8.9\text{ nm}^{-1}$ , which is independent from the methylene spacer length and thus represents the periodicity along one of the two lateral directions, presumably assigned to the distance between two DAP-units of adjacent polymer chains. These signals can be assigned to the (100) reflexes, whereby the corresponding second order peaks (200) with calculated distances of 0.35–0.36 nm represent the expected  $\pi$ - $\pi$ -interactions between the DAP-units, which are proven to be in the range of 0.33–0.38 nm,<sup>60</sup> indicating a parallel arrangement of the DAP-units of adjacent polymer chains. The broad signal in the wide angle range ( $14 \leq q \leq 16\text{ nm}^{-1}$ ), which is also independent from the methylene spacer length, can be assigned to the (110) reflex of an orthorhombic unit cell.<sup>58,61</sup> A closer inspection of the lamellar spacings calculated from the (001) diffraction peaks give  $d_{001}$  values of about 2.24 nm for a spacer length of  $n = 16$  (**7d**), 2.44 nm for  $n = 18$  (**7e**), and 2.64 nm for  $n = 20$  (**7f**), respectively. A linear dependence is observed if these distances are plotted as a function of the number of methylene units  $n$  [Fig. 5(b)]. An extrapolation of the  $d_{001}$  spacings to  $n = 0$  gives an intercept at about 6.3 Å, which corresponds to the size of the DAP layer in the lamellar structure. This value is close to theoretically calculated values for the size of a DAP group. Note that the linear dependence of the lamellar spacing  $d_{001}$  on the number of  $\text{CH}_2$  units  $n$  is a common feature which is commonly found for related polymers with linear methylene spacer in the main chain and also obtained for nanophase-separated comb-like polymers with lamellar morphology such as alkoxyated polyesters,<sup>62</sup> alkoxyated polyphenylene vinylenes,<sup>63</sup> and regio-regular poly(3-alkyl thiophenes)<sup>9</sup> wherein methylene sequences are part of the side chains. A slope of 1 Å per  $\text{CH}_2$  is observed for saturated DAP-polymers which is less than the ideal slope of 1.25 Å per  $\text{CH}_2$  expected for fully extended and interdigitated methylene sequences in the all-*trans* state without tilting. This indicates that there are features in saturated DAP polymers which are most likely a consequence of constraints caused by the DAP units.

### Crystal Structure Comparison of the Unprotected (**7c**) and Protected (**7f**) DAP Polymers and the Urea Polymer (**9**)

To compare the influence of different supramolecular interactions on the crystal structure, WAXS patterns of the unprotected (**7c**) and protected (**7f**) DAP-polymers as well as the urea polymer (**9**) with a methylene spacer length of  $n = 20$  were recorded after annealing them at  $40\text{ }^\circ\text{C}$ . The resulting diffraction patterns are shown in Figure 6. After annealing polymer **7f** shows a better resolved diffraction pattern. The

appearance of additional peaks in the wide angle range indicate the formation of a mixture of orthorhombic and triclinic crystal structures, also observed for precision polymers containing *meta*-substituted phenylenes.<sup>58</sup> By assigning the

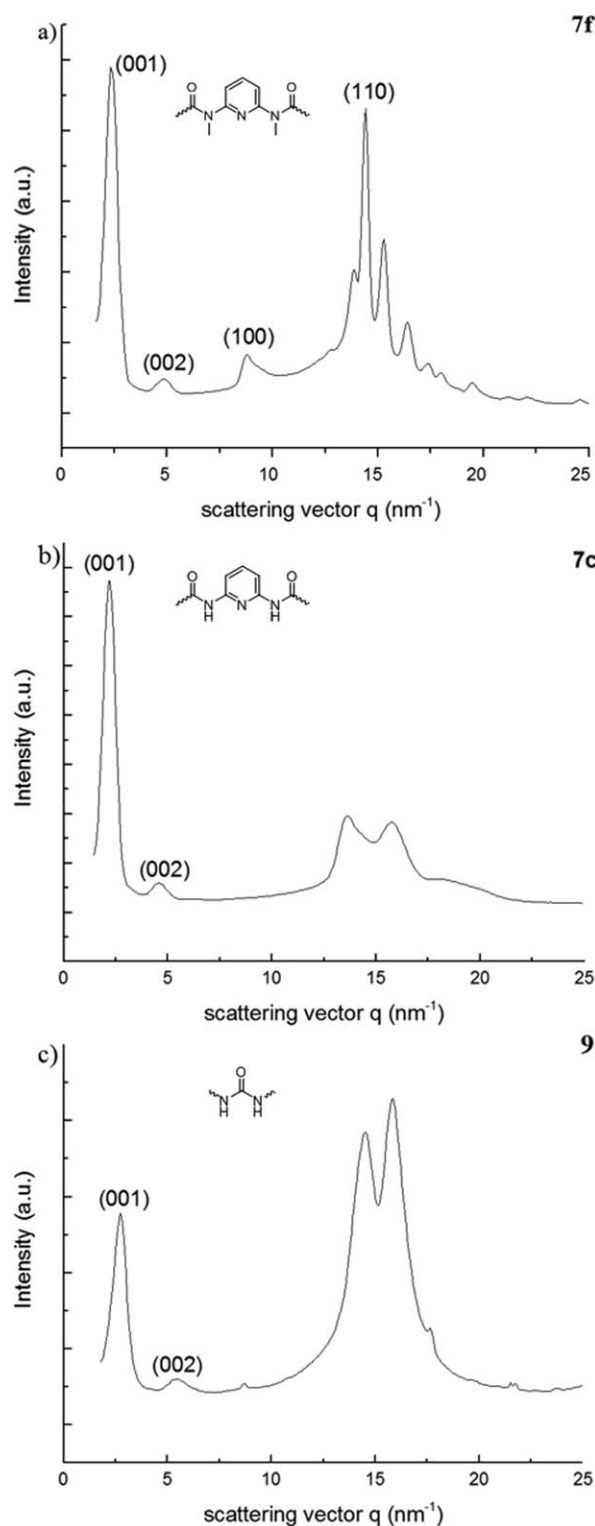


**FIGURE 6** X-ray diffraction patterns of the annealed (a) DAP polymer with methyl protection groups **7f**, (b) the DAP polymer without protection groups **7c**, and (c) the urea polymer **9**.

**TABLE 2** Unit Cell Parameters and Lamellar Crystal Thicknesses of the Saturated DAP Polymers (**7d–f**)

Code	<i>a</i> (nm)	<i>b</i> (nm)	<i>c</i> (nm)	<i>l<sub>c</sub></i> (nm)
<b>7d</b>	0.71	0.55	2.24	8.42
<b>7e</b>	0.71	0.55	2.44	12.11
<b>7f</b>	0.71	0.54	2.64	9.65

reflexes to the corresponding planes of an orthorhombic crystal cell (for **7d–f**), the calculation of the unit cell parameters, listed in Table 2, was possible.

The comparison of this parameters with those of orthorhombic PE (*a* = 0.74 nm, *b* = 0.49 nm)<sup>39,64</sup> shows a certain dilation of the unit cell in the direction of the *b*-axis. The X-ray diffraction pattern of the unprotected DAP-polymer **7c** [see Fig. 6(b)] also features two peaks in the low angle range, which represent the distance in the *c*-direction and can be assigned to the (001) and (002) reflex indicating the preservation of the lamellar morphology. Remarkable here is the disappearance of the signal at 8.9 nm<sup>-1</sup>, which indicates that the DAP-units are not arranged parallel to each other anymore. The polymer containing a urea-group (**9**) shows nearly the same diffraction pattern as the DAP-polymer without protection groups (**7c**) [see Fig. 6(c)]. The signals at 2.7 and 5.4 nm<sup>-1</sup> in the small angle range represent the (001) and (002) plane, thus implying a lamellar morphology, which was also observed in low-molecular weight urea-compounds interacting via hydrogen-bonding.<sup>65</sup> Another indication for the inclusion of the functional groups into the crystalline lamella (beside the dilation of the unit cell) is the lamellar thickness, which was calculated with the help of the Scherrer-equation (eq 2) given below

$$l_c = \frac{K \cdot \lambda}{\Delta(2\theta) \cdot \cos \theta_{hkl}} \quad (2)$$

where  $\Delta(2\theta)$  is the full peak width at half maximum height (FWHM),  $K \sim 1$  is the dimensionless Scherrer constant,  $\lambda = 0.154$  nm is the wavelength of the used Cu-K<sub>α</sub> radiation, and  $\theta_{hkl}$  is a Bragg angle of the relevant reflection.

If the functional group would be excluded from the crystal the lamellar crystal thickness would be equivalent to the length of the corresponding CH<sub>2</sub>-chain. Assuming an all-*trans* geometry we would expect a length of 1.88 nm for the C16-chain, 2.13 nm for C18, and 2.38 nm for C20. All of the calculated values for the lamellar crystal thickness, which range between 9.42 and 12.11 nm (see Table 2) exceeded these values, which further hints toward the inclusion of 3–5 functional groups into one crystal lamella.

## CONCLUSIONS

Series of polymers consisting of long methylene sequences with different functional groups (defects) placed at precisely regular intervals along the linear chain were synthesized via ADMET polymerization and subsequent hydrogenation using

TsNHNH<sub>2</sub>. By using Grubbs' 1st generation catalyst polymers with molecular weights ranging from 2700 to 10,000 g mol<sup>-1</sup> and polydispersity indices between 1.3 and 2.2 were obtained in good yields (68–97%). The thermal properties of all polymers (**6a–i**, **7a–i**, **8**, **9**) were investigated via DSC analysis, whereby the unprotected DAP polymers (**7a–c**) displayed melting temperatures, that are above pure ADMET-PE, explainable by enhanced thermal stability due to hydrogen bonds. The structure of selected polymers was analyzed using WAXD techniques. A lamellar morphology was observed for all the investigated polymers. Investigations on annealed samples of the saturated DAP polymer with 20 CH<sub>2</sub> units per methylene sequence indicated an orthorhombic unit cell, wherein the defects are at least partially included into the crystalline region.

#### ACKNOWLEDGEMENTS

The authors gratefully acknowledge the grant within the Sonderforschungsbereich SFB TRR 102 (Polymers under multiple constraints) (SR, WHB, Project A03) and (VD, MB, Project A15). Authors also thank Dr. Ute Baumeister, Matthias Fischer, and Nasir Mahmood for providing WAXS measurements.

#### REFERENCES AND NOTES

- 1 R. M. Michell, A. T. Lorenzo, A. J. Müller, M.-C. Lin, H.-L. Chen, I. Blaszczyk-Lezak, J. Martín, C. Mijangos, *Macromolecules* **2012**, *45*, 1517.
- 2 J. Martín, J. Maiz, J. Sacristan, C. Mijangos, *Polymer* **2012**, *53*, 1149.
- 3 H. Duran, M. Steinhart, H.-J. Butt, G. Floudas, *Nano Lett.* **2011**, *11*, 1671.
- 4 R. M. Michell, I. Blaszczyk-Lezak, C. Mijangos, A. J. Müller, *Polymer* **2013**, *54*, 4059.
- 5 R. M. Michell, A. J. Müller, *Prog. Polym. Sci.* **2016**, *54–55*, 183.
- 6 Y.-L. Loo, R. A. Register, A. J. Ryan, G. T. Dee, *Macromolecules* **2001**, *34*, 8968.
- 7 E. Hempel, H. Budde, S. Höring, M. Beiner, In *Progress in Understanding of Polymer Crystallization*; Reiter, G., Strobl, G. R., Eds.; Springer: Berlin, Heidelberg, **2007**; pp 201–228.
- 8 T. Babur, G. Gupta, M. Beiner, *Soft Matter* **2016**, *12*, 8093.
- 9 S. Pankaj, M. Beiner, *J. Phys. Chem. B* **2010**, *114*, 15459.
- 10 M. Ballauff, *Angew. Chem. Int. Ed.* **1989**, *28*, 253.
- 11 R. G. Alamo, K. Jeon, R. L. Smith, E. Boz, K. B. Wagener, M. R. Bockstaller, *Macromolecules* **2008**, *41*, 7141.
- 12 K. N. Bauer, H. T. Tee, I. Lieberwirth, F. R. Wurm, *Macromolecules* **2016**, *49*, 3761.
- 13 P. Kaner, C. Ruiz-Orta, E. Boz, K. B. Wagener, M. Tasaki, K. Tashiro, R. G. Alamo, *Macromolecules* **2013**, *47*, 236.
- 14 K. L. Opper, B. Fassbender, G. Brunklau, H. W. Spiess, K. B. Wagener, *Macromolecules* **2009**, *42*, 4407.
- 15 P. Ortmann, S. Mecking, *Macromolecules* **2013**, *46*, 7213.
- 16 G. Rojas, E. B. Berda, K. B. Wagener, *Polymer* **2008**, *49*, 2985.
- 17 G. Rojas, K. B. Wagener, *Macromolecules* **2009**, *42*, 1934.
- 18 G. Rojas, B. Inci, Y. Wei, K. B. Wagener, *J. Am. Chem. Soc.* **2009**, *131*, 17376.
- 19 M. D. Schulz, K. B. Wagener, *Macromol. Chem. Phys.* **2014**, *215*, 1936.
- 20 K. B. Wagener, J. T. Patton, *Macromolecules* **1993**, *26*, 249.
- 21 D. W. Smith, K. B. Wagener, *Macromolecules* **1993**, *26*, 1633.
- 22 J. E. O'Gara, J. D. Portmess, K. B. Wagener, *Macromolecules* **1993**, *26*, 2837.
- 23 J. T. Patton, J. M. Boncella, K. B. Wagener, *Macromolecules* **1992**, *25*, 3862.
- 24 K. Brzezinska, K. B. Wagener, *Macromolecules* **1992**, *25*, 2049.
- 25 K. B. Wagener, D. W. Smith, *Macromolecules* **1991**, *24*, 6073.
- 26 K. B. Wagener, K. Brzezinska, *Macromolecules* **1991**, *24*, 5273.
- 27 P. Atallah, K. B. Wagener, M. D. Schulz, *Macromolecules* **2013**, *46*, 4735.
- 28 J. Mandal, S. Krishna Prasad, D. S. S. Rao, S. Ramakrishnan, *J. Am. Chem. Soc.* **2014**, *136*, 2538.
- 29 M. Pulst, M. H. Samiullah, U. Baumeister, M. Prehm, J. Balko, T. Thurn-Albrecht, K. Busse, Y. Golitsyn, D. Reichert, J. Kressler, *Macromolecules* **2016**, *49*, 6609.
- 30 T. W. Gaines, E. B. Trigg, K. I. Winey, K. B. Wagener, *Macromol. Chem. Phys.* **2016**, *217*, 2351.
- 31 J. K. Leonard, Y. Wei, K. B. Wagener, *Macromolecules* **2011**, *45*, 671.
- 32 J. K. Leonard, T. E. Hopkins, K. Chaffin, K. B. Wagener, *Macromol. Chem. Phys.* **2008**, *209*, 1485.
- 33 G. Ungar, X.-B. Zeng, *Chem. Rev.* **2001**, *101*, 4157.
- 34 K. Yokota, *Prog. Polym. Sci.* **1999**, *24*, 517.
- 35 J. C. Sworen, J. A. Smith, K. B. Wagener, L. S. Baugh, S. P. Rucker, *J. Am. Chem. Soc.* **2003**, *125*, 2228.
- 36 H. S. Bazzi, H. F. Sleiman, *Macromolecules* **2002**, *35*, 9617.
- 37 M. D. Watson, K. B. Wagener, *Macromolecules* **2000**, *33*, 5411.
- 38 R. G. Alamo, L. Mandelkern, *Thermochim. Acta* **1994**, *238*, 155.
- 39 B. Inci, I. Lieberwirth, W. Steffen, M. Mezger, R. Graf, K. Landfester, K. B. Wagener, *Macromolecules* **2012**, *45*, 3367.
- 40 Y.-R. Zheng, H. T. Tee, Y. Wei, X.-L. Wu, M. Mezger, S. Yan, K. Landfester, K. Wagener, F. R. Wurm, I. Lieberwirth, *Macromolecules* **2016**, *49*, 1321.
- 41 X.-H. Dong, R. Van Horn, Z. Chen, B. Ni, X. Yu, A. Wurm, C. Schick, B. Lotz, W.-B. Zhang, S. Z. D. Cheng, *J. Phys. Chem. Lett.* **2013**, *4*, 2356.
- 42 K. E. Russell, D. C. McFaddin, B. K. Hunter, R. D. Heyding, *J. Polym. Sci. Part B: Polym. Phys.* **1996**, *34*, 2447.
- 43 G. Lieser, G. Wegner, J. A. Smith, K. B. Wagener, *Colloid Polym. Sci.* **2004**, *282*, 773.
- 44 W. Qiu, J. Sworen, M. Pyda, E. Nowak-Pyda, A. Habenschuss, K. B. Wagener, B. Wunderlich, *Macromolecules* **2005**, *39*, 204.
- 45 E. Boz, K. B. Wagener, A. Ghosal, R. Fu, R. G. Alamo, *Macromolecules* **2006**, *39*, 4437.
- 46 M. Tasaki, H. Yamamoto, M. Hanesaka, K. Tashiro, E. Boz, K. B. Wagener, C. Ruiz-Orta, R. G. Alamo, *Macromolecules* **2014**, *47*, 4738.
- 47 E. Boz, A. J. Nemeth, K. B. Wagener, K. Jeon, R. Smith, F. Nazirov, M. R. Bockstaller, R. G. Alamo, *Macromolecules* **2008**, *41*, 1647.

- 48** A. J. Heeger, *J. Phys. Chem. B* **2001**, *105*, 8475.
- 49** B. S. Ong, Y. Wu, P. Liu, S. Gardner, *J. Am. Chem. Soc.* **2004**, *126*, 3378.
- 50** X. Fang, K. Liu, C. Li, *J. Am. Chem. Soc.* **2010**, *132*, 2274.
- 51** S. Reimann, U. Baumeister, W. H. Binder, *Macromol. Chem. Phys.* **2014**, *215*, 1963.
- 52** C. Macleod, G. J. McKiernan, E. J. Guthrie, L. J. Farrugia, D. W. Hamprecht, J. Macritchie, R. C. Hartley, *J. Org. Chem.* **2002**, *68*, 387.
- 53** F. Saliu, B. Rindone, *Tetrahedron Lett.* **2010**, *51*, 6301.
- 54** H. Li, L. Caire da Silva, M. D. Schulz, G. Rojas, K. B. Wagener, *Polym. Int.* **2017**, *66*, 7.
- 55** K. Terada, E. B. Berda, K. B. Wagener, F. Sanda, T. Masuda, *Macromolecules* **2008**, *41*, 6041.
- 56** F. Marsico, M. Wagner, K. Landfester, F. R. Wurm, *Macromolecules* **2012**, *45*, 8511.
- 57** Z.-L. Li, L. Li, X.-X. Deng, L.-J. Zhang, B.-T. Dong, F.-S. Du, Z.-C. Li, *Macromolecules* **2012**, *45*, 4590.
- 58** S.-F. Song, Y.-T. Guo, R.-Y. Wang, Z.-S. Fu, J.-T. Xu, Z.-Q. Fan, *Macromolecules* **2016**, *49*, 6001.
- 59** S. Kobayashi, L. M. Pitet, M. A. Hillmyer, *J. Am. Chem. Soc.* **2011**, *133*, 5794.
- 60** C. Janiak, *J. Chem. Soc. Dalton Trans.* **2000**, 3885–3896.
- 61** B. Inci, K. B. Wagener, *J. Am. Chem. Soc.* **2011**, *133*, 11872.
- 62** T. Babur, J. Balko, H. Budde, M. Beiner, *Polymer* **2014**, *55*, 6844.
- 63** G. Gupta, V. Danke, T. Babur, M. Beiner, *J. Phys. Chem. B* **2017**, *121*, 4583.
- 64** M. Kobayashi, *J. Chem. Phys.* **1979**, *70*, 509.
- 65** M. George, G. Tan, V. T. John, R. G. Weiss, *Chem.—Eur. J.* **2005**, *11*, 3243.